

# PROCEEDINGS OF SPIE

[SPIDigitalLibrary.org/conference-proceedings-of-spie](https://SPIDigitalLibrary.org/conference-proceedings-of-spie)

## Nonlinear polymer/quantum dots nanocomposite for two-photon nanolithography of photonic devices

Abrashitova, Ksenia, Gulkin, Dmitry, Kokareva, Natalia, Safronov, Kirill, Chizhov, Artem, et al.

Ksenia A. Abrashitova, Dmitry N. Gulkin, Natalia G. Kokareva, Kirill R. Safronov, Artem S. Chizhov, Alexander A. Ezhov, Vladimir O. Bessonov, Andrey A. Fedyanin, "Nonlinear polymer/quantum dots nanocomposite for two-photon nanolithography of photonic devices," Proc. SPIE 10115, Advanced Fabrication Technologies for Micro/Nano Optics and Photonics X, 1011510 (20 February 2017); doi: 10.1117/12.2253179

**SPIE.**

Event: SPIE OPTO, 2017, San Francisco, California, United States

# Nonlinear polymer/quantum dots nanocomposite for two-photon nanolithography of photonic devices

Ksenia A. Abrashitova<sup>a</sup>, Dmitry N. Gulkin<sup>a</sup>, Natalia G. Kokareva<sup>a</sup>, Kirill R. Safronov<sup>a</sup>, Artem S. Chizhov<sup>b</sup>, Alexander A. Ezhov<sup>a</sup>, Vladimir O. Bessonov<sup>a</sup>, and Andrey A. Fedyanin<sup>a</sup>

<sup>a</sup>Faculty of Physics, Lomonosov Moscow State University, Moscow 119991, Russia

<sup>b</sup>Faculty of Chemistry, Lomonosov Moscow State University, Moscow 119991, Russia

## ABSTRACT

In this paper we report on fabrication of a nanocomposite based on CdSe quantum dots mixed with commercial photoresist ORMOCOMP and proved its high structurability by direct laser writing. The distribution of quantum dots was visualised by transmission electron microscopy and the quality and geometrical parameters of the structures were studied by optical and atomic force microscopy. We manufactured a novel photonic device for Bloch surface electromagnetic waves in photonic crystals and thoroughly studied their propagation by both leakage microscopy and back focal plane imaging methods. By z-scan method we measured the nonlinear Kerr coefficient of quantum dots. Its high value makes the manufactured photonic device promising for all-optical switching applications.

**Keywords:** two-photon lithography, direct laser writing, photonic crystals, Bloch surface waves, quantum dots, nonlinear optics

## 1. INTRODUCTION

Optical technology of data transfer has the advantage over electronic data transfer due to the higher / speed and less losses.<sup>1</sup> However, the bottleneck of the technology is the absence of fast all-optical switches. One of the ways to implement all-optical switching is based on nonlinear Kerr effect - the local modification of refractive index by an intense laser beam. The efficiency of switching depends on both the value of the nonlinear Kerr coefficient and the width of the resonance of the photonic switch. With the increase of nonlinear Kerr coefficient and the narrowing of the resonance, the efficiency of switching increases.

Bloch surface wave (BSW) in photonic crystal (PC) is an electromagnetic wave, propagating along and exponentially decaying away from the PC surface.<sup>2</sup> The BSW appears only in spectral ranges of the PC photonic bandgap.<sup>3</sup> BSWs in PCs confined in ultrathin polymeric stripes ( $\lambda/10$ ) possess excitation resonances few nanometers wide only,<sup>4</sup> that is important for all-optical switching applications. Furthermore, high concentration of electromagnetic field and the absence of ohmic losses make BSWs in PCs beneficial over surface plasmons.<sup>5</sup> There are only several works where the BSW confinement in polymeric stripes has been studied,<sup>6,7</sup> but no optical switches based on the BSW have been demonstrated so far. However, a BSW-supporting photonic structure must have well defined geometrical parameters. Thus one should carefully choose the method of structure fabrication.

Two-photon polymerization lithography (2PP) is a unique method of laser structuring. It is based on nonlinear absorption in focal volume and allows high resolution in three dimensions.<sup>8</sup> This lithographic method guarantees precise control of geometrical shape of manufactured structures which makes it an excellent candidate for the fabrication of BSW-supporting photonic structures. Unfortunately, third-order susceptibility of conventional photoresists is not large enough to observe optical Kerr effect and implement all-optical switching. A usual way to solve this problem is to mix photostructurable material with a highly nonlinear dopant.

---

Further author information: (Send correspondence to Ksenia A. Abrashitova)

Ksenia A. Abrashitova: E-mail: [abrashitova@nanolab.phys.msu.ru](mailto:abrashitova@nanolab.phys.msu.ru), Telephone: +7 (495) 939-45-44

Vladimir O. Bessonov: E-mail: [bessonov@nanolab.phys.msu.ru](mailto:bessonov@nanolab.phys.msu.ru), Telephone: +7 (495) 939-45-44

Nanocrystal quantum dots (QDs) are well known to have high values of optical nonlinearities,<sup>9</sup> but the QD structuring cannot reach optical-grade quality.<sup>10</sup> Mixing the QDs with photoresist allows one to obtain a nanocomposite with high optical nonlinearity without the loss of structurability.<sup>11</sup>

In this paper we present a composite based on the CdSe QDs with photocrosslinkable surface groups mixed with commercial photoresist ORMOCOMP. The composite has been structured via direct laser writing. The excitation of the BSW have been observed using optical spectroscopy and leakage radiation imaging experiments. The results of the back focal plane imaging coincide with numerical simulations and demonstrate the BSW coupling to a photonic device. Nonlinear-optical susceptibility of the QDs has been measured and its high value makes the fabricated photonic device attractive for all-optical switching.

## 2. EXPERIMENTAL TECHNIQUES AND DATA

The CdSe QDs have been manufactured according to the procedure suggested in the Ref.<sup>12</sup> : 0.1 mM of cadmium oleate, 0.1 mM of selenium dioxide, and 0.05 mM of oleic acid were mixed in a three-neck flask with 6.3 ml of 1-octadecene. The flask was vacuumed, heated with a constant velocity of 25 °C/min up to 240 °C and then left for 40 min. The reaction mixture was cooled down to the room temperature and the QDs precipitation has been conducted in a mixture of acetone and methanol. After that, the QDs were separated by centrifugation at 4000 rpm. After precipitation the QDs were washed with acetone, dried in air at 75 °C and redispersed in heptane.

According to Ref.<sup>13</sup> QDs suffer from the lack of dispersability in a polymer matrix. A chemical modification of QD surface groups may increase its compatibility with photoresist allowing a uniform dispersion of QDs in a polymer. The two-step surface group exchange reaction has been conducted as described in literature:<sup>14</sup> 200 mg of 11-mercaptoundecanethiol were added to 10 ml of nonaqueous ethanol and 15 ml of n-heptane and the mixture has been stirred until a clear solution was obtained. 10 mg of CdSe sol in n-heptane were added to the mixture and sonicated for 2 hours. The QD precipitated in chloroform and were separated by centrifugation at 4000 rpm. The nanocrystals were washed with n-heptane several times, dried in air at 75 °C and redispersed in 5 ml of dimethylsulfoxide (DMSO). 100  $\mu$ l of photopolymerisable 3-(trimethoxysilyl)propylmethacrylate has been added to the sol and the mixture has been kept at 50 °C for 10 hours in argon flow (20 ml/min). After the end of the reaction the QDs precipitated in 25 ml of chloroform, were separated by centrifugation, washed with n-heptane several times and dried in air at 75 °C.

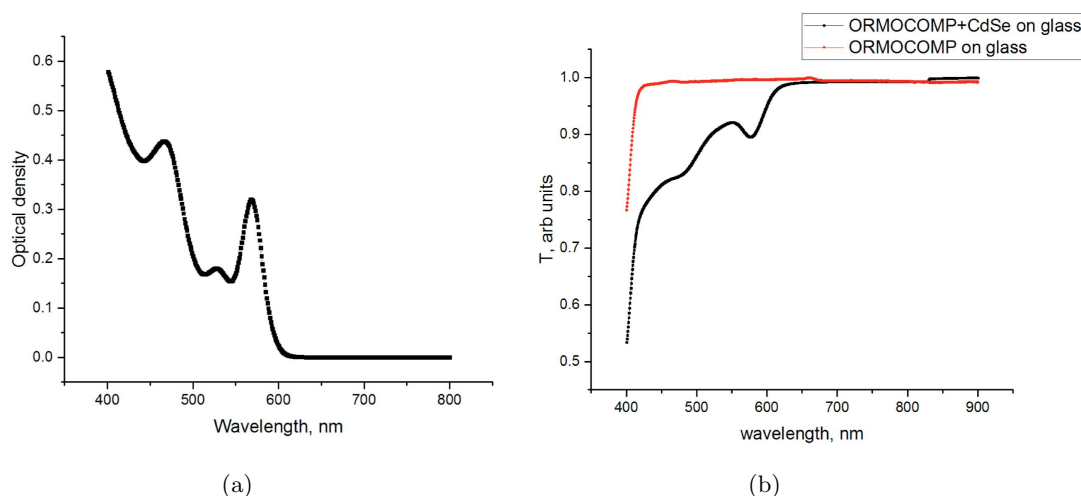


Figure 1: (a) Absorption spectrum of CdSe QDs in toluene. (b) Transmission spectrum of composite film ORMOCOMP+QD (black), compared to pure ORMOCOMP (red).

At first, we tried to mix the functionalized QDs directly with SU-8 and ORMOCOMP commercial photoresists. Unfortunately, the QDs seem to be only slightly soluble in ORMOCOMP and totally insoluble in the SU-8 solvent. We found experimentally that the functionalized QDs are well miscible in DMSO (solvent 1) and in 1:1

mixture of nonaqueous ethanol with methoxyethanol (solvent 2). By adding the QDs, dissolved in corresponding solutions, to photoresist clear and stable suspensions of the QDs in SU-8 as well as in ORMOCOMP were obtained. No visible precipitation was observed after 2 months. 8 mg of the QDs were redispersed in 0.5 ml of solvent 1 (sol 1) and in 0.6 ml of solvent 2 (sol 2). 0.034 g of SU-8 were added to 0.125 ml of sol 1. 0.09 ml of ORMOCOMP were added to sol 2. The obtained nanocomposites 1 and 2 were sonicated for 25 min, poured on a cover glass, dried at 95 and 85 °C respectively, for 30 min and exposed to UV lamp with a glass filter for 30 min. After that, sample 1 was additionally heated for 30 min at 95 °C, developed in mr-dev 600 for several hours, washed with isopropanol and dried. Sample 2 was developed in ORMODEV for several hours, washed with isopropanol and dried. The obtained concentration of QDs reaches 0.25 % in sample 1 and 0.23 % in sample 2.

The sol of the unmodified QDs in heptane was characterized by absorption spectroscopy in a wavelength range of 400-800 nm. Absorption spectrum has a well defined peak at 575 nm which corresponds to the QD mean size of approximately 3.7 nm<sup>15</sup> (figure 1a). A 100- $\mu$ m thick photocrosslinked composite (ORMOCOMP+QD) and pure ORMOCOMP photoresist samples were characterised by transmission spectroscopy in the wavelength range of 400-900 nm (figure 1b). An absorption peak at 580 nm wavelength of the composite film spectrum corresponds to the QD absorption and does not appear for a pure photoresist film of the same thickness. Two curves coincide in the wavelength range of 700 - 900 nm where the QDs are transparent.

For the further analysis dried films of samples 1 and 2 were sliced in ultramicrotome and were studied with a transmission electron microscopy (TEM) setup. TEM images have shown that the QDs form clusters both in sample 1 (figures 2c, 2d) and in sample 2 (figures 2a, 2b). The mean distance between clusters in sample 1 reaches several microns (figure 2c) and the mean cluster size is several hundreds of nanometers (figure 2d). In the second sample the QD clusters are of the same size (figure 2b), but are closer to each other: the mean distance between clusters is not more than 500 nm (figure 2a). One may notice that the QDs seem to be more incompatible with SU-8 than with ORMOCOMP. In nanocomposite 1 they form very densely packed clusters with the mean distance between them being larger than the characteristic geometrical parameters of the BSW-supporting photonic device. Hence in our further experiments we used nanocomposite 2 (QD+ORMOCOMP).

FDTD numerical simulations (Lumerical) demonstrated that the optimal waveguide height for BSW propagation is 200 nm. The simplest and the most reliable method to control structure height in this range is to expose 200 nm thin photoresist films. The thickness of the film may be controlled either by photoresist concentration or by the velocity of spin-coating. We used a standart spin-coating process and added ORMOTHIN to reduce the polymer concentration down to 30 % .

To perform photolithography we used a home-built 2PP-setup (figure 3). Laser radiation from the source (Ti:Sa femtosecond laser with the wavelength of 800 nm, 80 MHz repetition rate, 50 fs pulse duration) passed through the prism pulse precompressor (PPC) in order to compensate positive dispersion and maintain the pulse duration as short as possible. A system of half-wave plate in a motorized rotational stage (L/2), Glan-Taylor prism (GP1) and photodiode (PD) was used to control the power of radiation incident on the sample with the accuracy of tens of microwatts. Acoustooptic modulator (AOM) worked as a fast shutter and second Glan-Taylor prism (GP2) controlled the polarization of incident light. Fast steering mirror (FSM) moved beam in a sample plane with the accuracy of 1 nm in a field of 60  $\mu$ m x 60  $\mu$ m. Laser beam was expanded by the telescope to completely cover the entrance aperture of the focusing air objective (NA = 0.95, magnification = 100x). The objective was mounted on a piezostage (PS) that provided the movement of the beam along the objective optical axis Z with a maximum travel range of 200  $\mu$ m and accuracy of 5 nm . The sample was mounted on a microscope table (MT) that provided long-distance travel in the sample surface plane XY with a travel range of 11.5 cm in X and 7.5 cm in Y and the accuracy of 100 nm. CMOS camera (CAM) visualised the process of polymerization and was used to measure and compensate sample tilt. The 2PP setup was completely automatic.



in comparison to prism schemes and added focusing and defocusing triangles in order to increase the efficiency of the BSW insertion and extraction. Hence, our BSW-supporting photonic device consisted of an entrance diffraction grating, a focusing triangle, a waveguide, a defocusing triangle and an exit diffraction grating. In order to increase the resolution and reach desired geometrical parameters, the speed of the moving beam waist and the power of incident radiation were optimized. The quality of fabricated structures was monitored by optical microscopy (figure 4a) and then were studied by an atomic force microscopy (AFM) (figure 4b, figure 4c). The geometrical parameters for a photonic structure have been chosen as follows: waveguide length of 20  $\mu\text{m}$ , diffraction grating period of 1340 nm and waveguide width of 2  $\mu\text{m}$ .

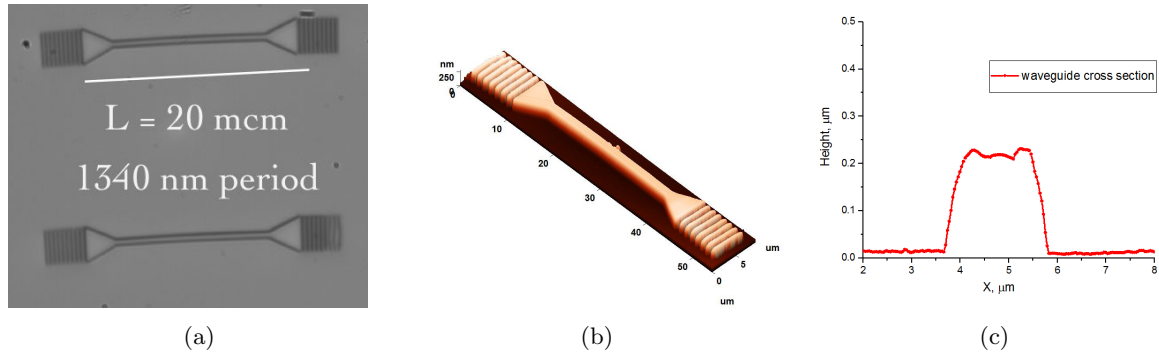


Figure 4: (a) Optical micrograph of the photonic device. (b) AFM image of the photonic device. (c) Crosssection of a waveguide.

The light propagation in the photonic device was studied by methods of the leakage radiation (LR) microscopy and the back focal plane (BFP) imaging (figure 5). Ti:Sa femtosecond laser (800 nm, 80 MHz, 50 fs) and laser diodes (wavelengths of 670, 780 and 850 nm) were used as light sources. A system of Glan-Taylor prism (GP1) and half-wave plate ( $\lambda/2$ ) in a precise rotational mount were used to control the power and polarization of the incident radiation. An air objective with numerical aperture of 0.5 focused the light to a sample and the transmitted LR was collected by oil-immersion objective with  $\text{NA}=1.3$ . Two objectives and the sample were mounted on independent precise 3-axis stages. The second Glan-Taylor prism (GP2) was used to control the polarization of the light transmitted through the sample. An iris diaphragm (D1) cut the parasitic background and was used to suppress the light scattered from the entrance diffraction grating. A slit (S1) with adjustable width was mounted on a translational stage and cut different reflexes on the BFP image. The BFP image was visualised by CMOS camera CAM1 and the direct image was visualised by CMOS camera CAM2. The spectrum of a transmitted light was measured by a spectrometer.

The image of the LR (figure 6a on the left) shows that the photonic device is able to guide light. Transmission spectrum of the structure (figure 6b) illuminated by a broadband lightsource demonstrates a qualitative agreement with numerical simulations made using the FDTD technique. All these experiments, however, do not directly demonstrate the BSW excitation and propagation in the photonic device. Hence we provided additional BFP experiment to study the mode structure of the transmitted light. The BFP image (figure 6a on the right) shows three bright stripes corresponding to three modes supported by the fabricated photonic device. The modes' effective refractive indices from the BFP image and the obtained values coincide with the FDTD results (1.19, 1.10, 1.01).

The nonlinearity of QDs diluted in DMSO was measured using a standard z-scan technique.<sup>16</sup> A laser beam from a low repetition rate femtosecond laser (Ti:Sa, 800 nm wavelength, 1 KHz repetition rate, 50 fs pulse duration) was narrowed down by a telescope to fit the entrance aperture of two Glan-Taylor prisms that controlled the power and polarization of the light incident at a sample. A long-focus lens (100 mm) focused the beam inside a sample and after passing through the sample the beam was divided in two channels by a beam splitter. In a first channel the beam passed through the adjustable aperture and then was focused to the photodetector while in the second channel all the transmitted light was directly focused to another photodetector. The sample was mounted on a motorized translational stage. The signals collected from the photodetectors were averaged by



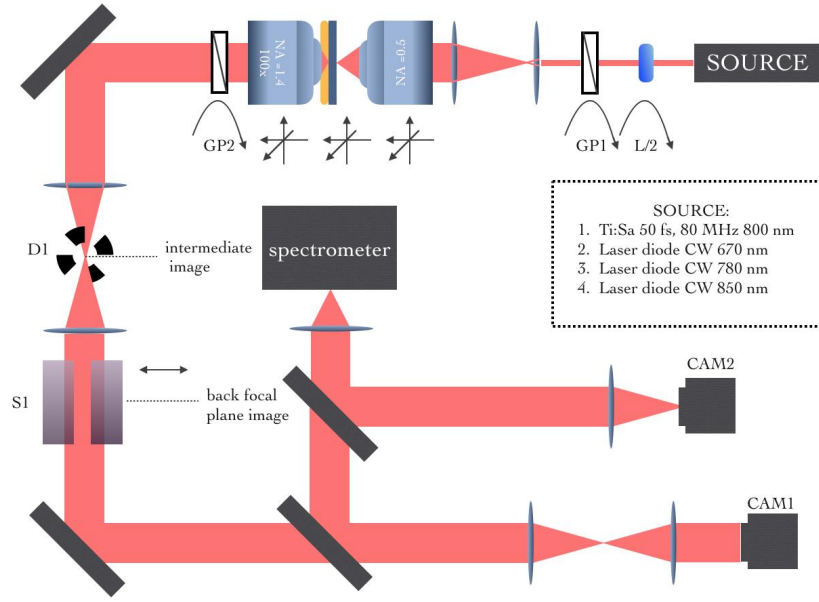


Figure 5: The LR and BFP imaging setup principle scheme.

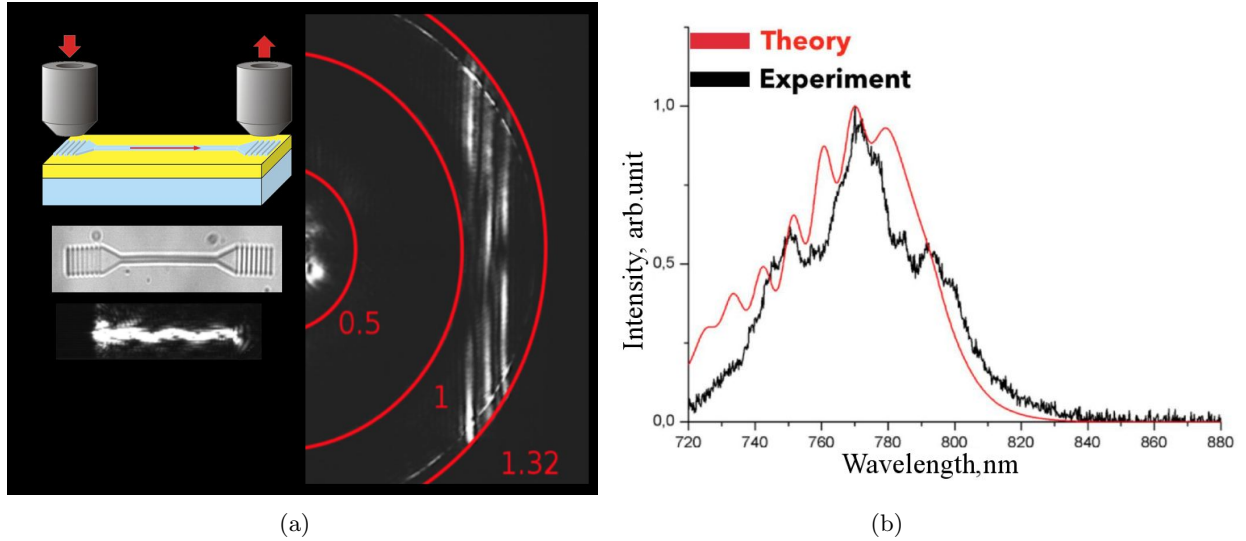


Figure 6: (a) The BFP image and the LR image. (b) Spectrum of light transmitted through the photonic device.

a boxcar and digitized. The final curve has been calculated as the normalized aperture-channel transmittance divided by the non-aperture-channel transmittance. The results are presented in figure 7. The curve showed standard peak-valley form which indicated positive Kerr nonlinearity. We used the standard formulas by Sheik-Bahae<sup>17</sup>  $|\Phi_0| = \Delta T_{pv}/0.406(1 - S)^{0.27}$ ,  $n_2 = (\frac{\lambda}{2\pi})\Phi_0/I_0 L_{eff}$ , where  $|\Phi_0|$  is the on-axis peak nonlinear phase shift generated by the sample placed at the lens focus,  $\Delta T_{pv}$  is the normalized transmittance between peak and valley,  $\lambda$  is the wavelength of incident radiation,  $S$  is the fraction of the beam transmitted through the aperture,  $I_0$  is the peak irradiance in the focus and  $L_{eff}$  is considered to be the sample width for transparent samples. The nonlinear Kerr coefficient of the QDs  $n_2$  was estimated to be  $10^{-13} \text{ cm}^2/\text{W}$  which is 3 orders of magnitude larger than  $n_2$  of silica glass.

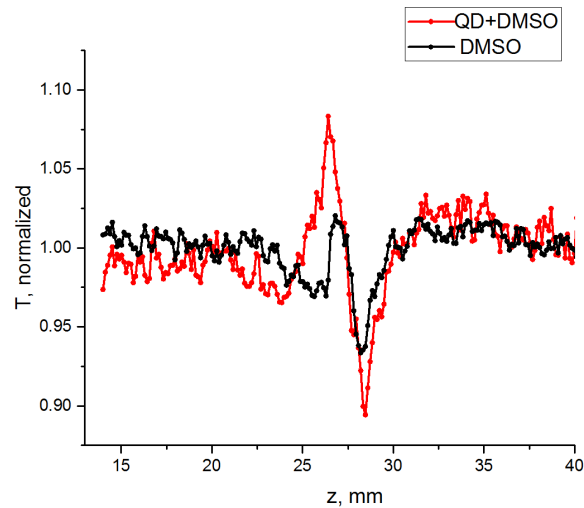


Figure 7: Z-scan curve for QDs in DMSO and pure DMSO.

### 3. CONCLUSIONS

In our work we fabricated a novel BSW-supporting photonic device from the composite photoresist ORMOCOMP mixed with the CdSe QDs. The transmission capabilities of a device and the mode structure of confined light has been analysed by the LR microscopy and the BFP imaging methods. The optical nonlinearity of QDs has been measured by z-scan technique. Its value reaches  $10^{-13} \text{ cm}^2/\text{W}$ . The demonstrated properties of fabricated device open new possibilities in the field of all-optical switching.

### ACKNOWLEDGMENTS

This work was partially supported by the Russian Foundation for Basic Research (15-32-70021) (measurements of optical and nonlinear optical properties) and the Russian Science Foundation (Grant No. 15-12-00065) (sample fabrication and characterization).

### REFERENCES

- [1] Alduino, A. and Paniccia, M., "Interconnects: Wiring electronics with light," *Nature Photonics* **1**(3), 153–155 (2007).
- [2] Yeh, P., Yariv, A., and Hong, C.-S., "Electromagnetic propagation in periodic stratified media. I. General theory," *J. Opt. Soc. Am. A* **67**(4), 438 (1977).
- [3] Yeh, P., Yariv, A., and Cho, A. Y., "Optical surface waves in periodic layered media," *Appl. Phys. Lett.* **32**(2), 104–105 (1978).
- [4] Descrovi, E., Giorgis, F., Dominici, L., and Michelotti, F., "Experimental observation of optical bandgaps for surface electromagnetic waves in a periodically corrugated one-dimensional silicon nitride photonic crystal," *Opt. Lett.* **33**(3), 243 (2008).
- [5] Sinibaldi, A., Danz, N., Descrovi, E., Munzert, P., Schulz, U., Sonntag, F., Dominici, L., and Michelotti, F., "Direct comparison of the performance of Bloch surface wave and surface plasmon polariton sensors," *Sensors and Actuators, B: Chemical* **174**, 292–298 (2012).
- [6] Descrovi, E., Sfez, T., Quaglio, M., Brunazzo, D., Dominici, L., Michelotti, F., Herzig, H. P., Martin, O. J. F., and Giorgis, F., "Guided bloch surface waves on ultrathin polymeric ridges," *Nano Letters* **10**(6), 2087–2091 (2010).
- [7] Sfez, T., Descrovi, E., Yu, L., Brunazzo, D., Quaglio, M., Dominici, L., Nakagawa, W., Michelotti, F., Giorgis, F., Martin, O. J. F., and Herzig, H. P., "Bloch surface waves in ultrathin waveguides: near-field investigation of mode polarization and propagation," *J. Opt. Soc. Am. B* **27**(8), 1617 (2010).



- [8] Malinauskas, M., Farsari, M., Piskarskas, A., and Juodkazis, S., “Ultrafast laser nanostructuring of photopolymers: A decade of advances,” *Phys. Rep.* **533**(1), 1–31 (2013).
- [9] Gerdova, I. and Haché, A., “Third-order non-linear spectroscopy of CdSe and CdSe/ZnS core shell quantum dots,” *Opt. Comm.* **246**(1-3), 205–212 (2005).
- [10] Xu, B.-B., Zhang, Y.-L., Zhang, R., Wang, L., Xiao, X.-Z., Xia, H., Chen, Q.-D., and Sun, H.-B., “Programmable assembly of CdTe quantum dots into microstructures by femtosecond laser direct writing,” *J. Mat. Chem. C* **1**(31), 4699 (2013).
- [11] Jia, B., Buso, D., Van Embden, J., Li, J., and Gu, M., “Highly non-linear quantum dot doped nanocomposites for functional three-dimensional structures generated by two-photon polymerization,” *Adv. Mat.* **22**(22), 2463–2467 (2010).
- [12] Chen, O., Chen, X., Yang, Y., Lynch, J., Wu, H., Zhuang, J., and Cao, Y. C., “Synthesis of metal-selenide nanocrystals using selenium dioxide as the selenium precursor,” *Angewandte Chemie - International Edition* **47**(45), 8638–8641 (2008).
- [13] Balazs, A. C., Emrick, T., and Russell, T. P., “Nanoparticle Polymer Composites: Where Two Small Worlds Meet,” *Science* **314**(5802), 1107–1110 (2006).
- [14] Krini, R., Ha, C. W., Prabhakaran, P., Mard, H. E., Yang, D.-Y., Zentel, R., and Lee, K.-S., “Photosensitive Functionalized Surface-Modified Quantum Dots for Polymeric Structures via Two-Photon-Initiated Polymerization Technique,” *Macromolecular Rapid Communications*, 1108–1114 (2015).
- [15] Jasieniak, J., Smith, L., Van Embden, J., Mulvaney, P., and Califano, M., “Re-examination of the size-dependent absorption properties of CdSe quantum dots,” *J. Phys. Chem. C* **113**(45), 19468–19474 (2009).
- [16] Stryland, E. W. V. and Sheik-Bahae, M., “Z-Scan Measurements of Optical Nonlinearities,” *Characterization Techniques and Tabulations for Organic Nonlinear Materials* (3), 655–692 (1998).
- [17] Sheik-Bahae, M., Said, A. A., Wei, T.-H., Hagan, D. J., and Van Stryland, E. W., “Sensitive measurement of optical nonlinearities using a single beam,” *IEEE J. Quant. Electron.* **26**(4), 760–769 (1990).